Dirac Field in FRW Spacetime: Current and Energy Momentum

P.R. Dhungel and U. Khanal
Central Department of Physics, Tribhuvan University, Kirtipur, **Nepal**

August 15, 2012

Abstract

The behaviour of the Dirac field in FRW space-time is investigated. The relevant equations are solved to determine the particle and energy distribution. The angular and radial parts are solved in terms of Jacobi polynomials. The time dependence of the massive field is solved in terms of known function only for the radiation filled flat space. WKB method is used for approximate solution in general FRW space. Of the two independent solutions, one is found to decay in time as the Universe expands, while the other solution grows. This could be the source of the local particle current. The behaviour of the particle number and energy density are also investigated. It is found that the particles arrange themselves in a number and density distribution pattern that produces a constant Newtonian potential as required for the flat rotation curves of galaxies. Further, density contrast is found to grow with the expansion.

PACS: 03.65.Pm, 04.20.Cv, 04.98.80.Jk
Keywords: Dirac equation, NP formalism, FRW space-time, Spinors.

1 Introduction

Since all matter is ultimately fermionic, behaviour of Dirac field in expanding Universe must reveal hitherto unknown features of the Universe. The properties of matter fields in general, and the massive Dirac fields in particular, must have profound consequences on the structure formation proecess.

The spinor formalism developed by B. v. d. Waerden[1] in 1928 and later elaborated by O. Laporte, et al comprises all representations of the Lorentz group, even those not contained in ordinary tensor analysis. However, it was not widely used at that time. Later, in 1936, the spinor calculus was used by Dirac[4] to derive wave equations for particles with spin greater than one half, that means wave equations for (elementary) particles that had not been discovered up to then. This made the spinor calculus known to a wider audience and Brill and Wheeler's [5]analysis and application to the interaction of neutrinos with gravitational fields further added weights to this. When Newman and Penrose

developed a special formalism[6] of projecting vectors, tensors and spinors onto a set of null tetrad bases (explained in detail in Ref. [7]), it became a very useful tool to study the behaviour of quantum-fields of all spins in general relativistic back-ground gravity. This method has been used successfully in various black hole geometries [7, 8, 9, 11] and more recently to further study the behaviour of Dirac particles in different geometries [12, 13, 14, 15, 16].

In continuance of previous work [17, 18] on applying this method to investigate the behaviour of the fields of electrodynamics in Friedmann-Robertson-Walker(FRW) space-time, we take up the Dirac field to get some insight on the process of structure formation. For our purpose, we first write the metric as [19, 20]

$$ds^2 = a^2\left[d\eta^2 - dr^2 - S^2\left(d\theta^2 + \sin^2\theta d\phi^2\right)\right] \tag{1}$$

where a is the scale factor that depends on the conformal time η which is related to the cosmic co-moving time t by $dt = ad\eta$, and

$$S = \frac{\sin\left(\sqrt{K}r\right)}{\sqrt{K}} = \begin{cases} \sin r, & K = 1 \\ r, & K = 0 \\ \sinh r, & K = -1 \end{cases} . \tag{2}$$

The flat case can be considered to be the limit of either the closed or open cases for $K \to 0$. Thus, in the complexified r-plane, the closed Universe lies along the real axis, open along the imaginary and flat near the origin. So, we may consider the proposition that, as an overall flat space expands, it fragments into under-density voids that develop locally as an open FRW space along the imaginary axis, and the overdensity regions evolve locally into the large scale structures as the closed counterpart. We choose the null tetrad as $l_\mu = [1, -1, 0, 0]$, $n_\mu = \frac{a^2}{2}[1, 1, 0, 0]$, $m_\mu = -\frac{aS}{\sqrt{2}}[0, 0, 1, i\sin\theta]$ and the complex conjugate $\bar{m}_\mu$so that the directional derivatives can be expressed as

$$\begin{aligned} D = l^\mu\partial_\mu \quad &= \tfrac{1}{a^2}\mathcal{D}_-, \quad \Delta = n^\mu\partial_\mu - \frac{1}{2}\mathcal{D}_+ \\ \delta = m^\mu\partial_\mu \quad &= \tfrac{1}{\sqrt{2}aS}\mathcal{L}_-, \quad \delta^* = \bar{m}^\mu\partial_\mu = \frac{1}{\sqrt{2}aS}\mathcal{L}_+ \end{aligned} \tag{3}$$

where,

$$\mathcal{D}_\pm \quad = \quad \frac{\partial}{\partial r} \mp \frac{\partial}{\partial \eta} \tag{4}$$

and

$$\mathcal{L}_\pm = \frac{\partial}{\partial\theta} \mp \frac{i}{\sin\theta}\frac{\partial}{\partial\phi} \tag{5}$$

The spinor equivalent of these directional derivatives are

$$\partial_{00'} = D, \quad \partial_{11'} = \Delta, \quad \partial_{01'} = \delta, \quad and \quad \partial_{10'} = \delta^* \tag{6}$$

Also, the non-vanishing spin coefficients [7] are given by $\beta = -\alpha = \frac{\cot\theta}{2\sqrt{2}S}$, $\gamma = -\frac{1}{2a}\frac{\partial a}{\partial \eta}$, $2\mu = \frac{1}{a}\frac{\partial a}{\partial \eta} - \frac{1}{S}\frac{\partial S}{\partial r}$, $-a^2\rho = \frac{1}{a}\frac{\partial a}{\partial \eta} + \frac{1}{S}\frac{\partial S}{\partial r}$.

Dirac equations for spin-1/2 particles represented by a pair of spinors, P^A and $\bar{Q}^{A'}$, are

$$\sigma^i{}_{AB'}\partial_i P^A + i\frac{M}{\sqrt{2}}\bar{Q}_{B'} = 0 \tag{7}$$

and

$$\sigma^i{}_{AB'}\partial_i Q^A + i\frac{M}{\sqrt{2}}\bar{P}_{B'} = 0, \tag{8}$$

where $\sigma^i{}_{AB'}$ are Pauli-martices and M is the mass of the particle (expressed as the inverse of its Compton wave-length). To write these equations in the Newman-Penrose formalism in a curved space-time, we replace the ordindary derivatives with covariant derivatives and Pauli-matrices by σ generalized to curved spacetime as

$$\sigma^i{}_{AB'} = \frac{1}{\sqrt{2}}\begin{vmatrix} l^i & m^i \\ \bar{m}^i & n^i \end{vmatrix} \tag{9}$$

Thus the Dirac equations are

$$\sigma^i{}_{AB'}P^A{}_{;\,i} + i\frac{M}{\sqrt{2}}\bar{Q}^{C'}\varepsilon_{C'B'} = 0 \tag{10}$$

and

$$\sigma^i{}_{AB'}Q^A{}_{;\,i} + i\frac{M}{\sqrt{2}}\bar{P}^{C'}\varepsilon_{C'B'} = 0, \tag{11}$$

where

$$\varepsilon_{C'B'} = \begin{vmatrix} 0 & 1 \\ -1 & 0 \end{vmatrix} \tag{12}$$

In order to write explicit forms of these equations in terms of spin coefficients, consider the case $B' = 0$ in Eq. (10):

$$\sigma^i{}_{00'}P^0{}_{;\,i} + \sigma^i{}_{10'}P^1{}_{;\,i} - i\frac{M}{\sqrt{2}}\bar{Q}^{1'} = 0, \tag{13}$$

Explicitly, in NP formalism this becomes

$$(\partial_{00'}P^0 + \Gamma^0{}_{d00'}P^d) + (\partial_{10'}P^1 + \Gamma^1{}_{d10'}P^d) = i\frac{M}{\sqrt{2}}\bar{Q}^{1'} \tag{14}$$

Noting that $\Gamma^1 = \varepsilon^{10}\Gamma_0 = -\Gamma_0$ and $\Gamma^0 = \varepsilon^{01}\Gamma_1 = \Gamma_1$and using (6), this equation can be written as

$$DP^0 + (\Gamma_{1000'}P^0 + \Gamma_{1100'}P^1) + \delta^* P^1 - (\Gamma_{0010'}P^0 + \Gamma_{0110'}P^1) = i\frac{M}{\sqrt{2}}\bar{Q}^{1'} \quad (15)$$

Replacing the various spin coefficient by their special symbols [7], we obtain

$$(D + \varepsilon - \rho)P^0 + (\delta^* + \pi - \alpha)P^1 = i\frac{M}{\sqrt{2}}\bar{Q}^{1'} \quad (16)$$

Similarly, for $B' = 1$ in Eq. (10) gives another such equation and following the similar steps with the complex conjugate of Eq. (11) gives the other two equations. Hence the Dirac equations for the components of the Dirac spinors in NP formalism are given by

$$\begin{aligned}
(D + \varepsilon - \rho)P^0 + (\delta^* + \pi - \alpha)P^1 &= i\frac{M}{\sqrt{2}}\bar{Q}^{1'}, \\
(\Delta + \mu - \gamma)P^1 + (\delta + \beta - \tau)P^0 &= -i\frac{M}{\sqrt{2}}\bar{Q}^{0'}, \\
(D + \varepsilon^* - \rho^*)\bar{Q}^{0'} + (\delta + \pi^* - \alpha^*)\bar{Q}^{1'} &= -i\frac{M}{\sqrt{2}}P^1, \ \textit{and} \\
(\Delta + \mu^* - \gamma^*)\bar{Q}^{1'} + (\delta^* + \beta^* - \tau^*)\bar{Q}^{0'} &= i\frac{M}{\sqrt{2}}P^0. \quad (17)
\end{aligned}$$

In the next section, the solution of these equations including angular, radial and time parts are presented. Section 3 deals with the particle current and the energy-momentum of the field. Concluding remarks are made in the last section. Although the solutions of Dirac equations have been obtained earlier [21, 22, 23, 24], they are either restricted to some special cases or the expressions are comparatively complex ones. With our choice of null tetrad bases, the separated equations are more tractable and the solutions can be written in terms of known mathematical functions.

2 Solutions

Substituting ($\sqrt{2}SaP^0$, Sa^2P^1, $-\sqrt{2}Sa\bar{Q}^{0'}$, $Sa^2\bar{Q}^{1'}$) with

($\phi_{-1/2}Y_{-1/2}$, $\phi_{1/2}Y_{1/2}$, $\phi_{-1/2}Y_{1/2}$, $\phi_{1/2}Y_{-1/2}$) in the Eqs. (17), using the directional derivatives and spin-coefficients given in Sec. 1, the angular parts of Eqs. (17) are found to separate into

$$\left(\mathcal{L}_\pm + \frac{1}{2}\cot\theta\right) Y_{\pm 1/2} = \mp\lambda Y_{\mp 1/2}, \quad (18)$$

while the radial and time parts satisfy

$$r\mathcal{D}_\pm \phi_{\pm 1/2} = (f\lambda \mp iMra)\,\phi_{\mp 1/2} \quad (19)$$

Substituting for $Y_{+1/2} = \left(\mathcal{L}_- + \frac{1}{2}\cot\theta\right) Y_{-1/2}$from Eq. (18) into the one for $Y_{-1/2}$, and a similar process with $Y_{-1/2}$, gives us the two angular equations

$$\left(\frac{1}{\sin\theta}\frac{\partial}{\partial\theta}\sin\theta\frac{\partial}{\partial\theta} \pm \frac{i\cos\theta}{\sin^2\theta}\frac{\partial^2}{\partial\varphi^2} - \frac{1}{4}\cot^2\theta - \frac{1}{2}\lambda^2\right) Y_{\pm 1/2} = 0 \qquad (20)$$

Explicitly, the angular parts representing the two helicities are solved in terms of the Jacobi polynomials $P_n^{(\alpha,\beta)}$ given by the spin weighted spherical harmonics

$${}_{\pm s}Y_l^m(\theta,\phi) = Ne^{im\phi}(1-\cos\theta)^{\frac{m}{2}\pm\frac{s}{2}}(1+\cos\theta)^{\frac{m}{2}\mp\frac{s}{2}}P_{l-m}^{(m\pm s, m\mp s)}(\cos\theta) \qquad (21)$$

of spin weight $s = \frac{1}{2}$; here, the total angular momentum $l = s+1, s+2, ...,$ are half-integers as they already include the spin and the separation constant $\lambda = (l+1/2)$. ${}_{\pm s}Y_l^m$ are appropriately normalized and weighted to give $\int_{\theta=0}^{\pi}\int_{\phi=0}^{2\pi} {}_sY_{l'}^{m'*}{}_sY_m^l \sin\theta d\theta d\phi = \delta_{ll'}\delta_{mm'}$. The radial and temporal parts can also be separated by writing $R_\pm T_\pm = \phi_{1/2} \pm \phi_{-1/2}$ in Eq. (19) to give the equations

$$\frac{1}{R_\mp}\left(\frac{\partial}{\partial r} \mp \frac{l+1/2}{S(r)}\right) R_\pm = \frac{1}{T_\pm}\left(\frac{\partial}{\partial\eta} \pm iMa\right) T_\mp = ik. \qquad (22)$$

The separation constant $k = pa$ can be identified with the comoving momentum. The solutions labeled $\pm$ can be decoupled easily[17], and we believe that they represent the negative and positive energy solutions respectively. The decoupled equatins are of second order and are given by

$$\left(\frac{\partial}{\partial r} \pm \frac{l+1/2}{S(r)}\right)\left(\frac{\partial}{\partial r} \mp \frac{l+1/2}{S(r)}\right) R_\pm = -k^2 R_\pm \qquad (23)$$

and

$$\left(\frac{\partial}{\partial\eta} \pm iMa\right)\left(\frac{\partial}{\partial\eta} \mp iMa\right) T_\pm = -k^2 T_\pm. \qquad (24)$$

2.1 Radial Solutions

The resulting regular radial solutions

$$\begin{aligned} R_\pm &= A_\pm \left(1-\cos\sqrt{K}r\right)^{\frac{l+1}{2}\mp\frac{1}{4}} \left(1+\cos\sqrt{K}r\right)^{\frac{l+1}{2}\pm\frac{1}{4}} \\ &\quad P_{\frac{k}{\sqrt{K}}-l-1}^{\left(l+\frac{1}{2}\mp\frac{1}{2},\frac{l}{2}+\frac{1}{2}\pm\frac{1}{2}\right)}\left(\cos\sqrt{K}r\right), \end{aligned} \qquad (25)$$

are the appropriately weighted Jacobi polynomials that can be normalized to give $\int_0^\pi |R_\pm|^2 dr = 1$. The behaviour of $R_\pm$ is displayed in Fig. (1). It suffices to write the radial solutions for all $K's$ in the form of Eq.(25), as the limit to

flat space is achieved with $K \to 0$, in which case the asymptotic behaviour of the Jacobi polynomial of large order leads to [25]

$$R_{\pm} = A_{\pm} r j_{l \mp \frac{1}{2}}(kr) \tag{26}$$

where j_n are the spherical Bessel functions. It was shown in Ref. [17] that $R_+^* R_- = -R_+ R_-^*$, so that $A_- = iA_+$. As the mass does not appear in the radial solution, the spatial solution of the massive and massless field equations are the same. The mass couples with the scale factor and appears only in the temporal part. One important aspect of the solution Eq. (25) is that $k - l - 1 = n$ has to be an integer for $R_{\pm}$ to be regular at $r = 0$ and π. As $l \geq \frac{1}{2}$ is a half-integer increasing in steps of unity from its minimum value, $k \geq \frac{3}{2}$ is also half-integer. Hence, the momentum of the free Dirac field in closed FRW spacetime is quantized in steps of unity from $\frac{3}{2}$ upwards. This minimum value of $\frac{3}{2}$ can be interpreted as half unit of spin and one unit representing the mass in the lowest momentum state for the massive or one unit of lightlike momentum for the massless fields. Eq (22) leads to a number of Wronskian-like conditions, the most important of which that we will require later are

$$\begin{aligned} |T_+|^2 + |T_-|^2 &= 1 \\ ik\left[T_+^* T_- - T_+ T_-^*\right] &= \frac{d}{d\eta}|T_+|^2 \\ ik\left[|R_+|^2 - |R_-|^2\right] &= \frac{d}{dr} R_+^* R_- = -\frac{d}{dr} R_+ R_-^*. \end{aligned} \tag{27}$$

2.2 Time Evolution

The decoupled temporal equation is

$$\left(\frac{d^2}{d\eta^2} + k^2 + M^2 a^2 \mp iMa'\right) T_{\pm} = 0, \tag{28}$$

and $a'^2 = \left(\frac{da}{d\eta}\right)^2 = H_0^2\left[\Omega_\Lambda a^4 + (1 - \Omega_\Lambda - \Omega_M - \Omega_R)\, a^2 + \Omega_M a + \Omega_R\right]$ is given by the Friedmann-Le Maitre equation with Ω_Λ, Ω_M and Ω_R being the densities contributed by the cosmological constant, matter and radiation respectively, in units of the critical density at the time η_0 when the scale factor is normalized to $a_0 = 1$. Given a functional form for $a(\eta)$, it is always possible to write a series solution[18] of Eq.(28). It is instructive to start with solutions for the massless field. The two solutions are just

$$T_{\pm} = \pm \frac{1}{\sqrt{2}} e^{-ik\eta}, \tag{29}$$

where the multiplicative constants and their signs have been fixed by the conditions imposed by Eqs. (22) and (27).

As shown in Ref. [17], the time dependence can be solved in terms of a known special function (Whitaker) only in the case of the radiation filled flat

Universe. This case is very important for the reason that it represents the nature of the early radiation dominated Universe from the very big-bang during which time, the density parameter was extremely fine-tuned to almost unity. So before trying to approximate the general solution, let us consider this in some further details. The solutions are better represented in terms of the parabolic cylinder functions[26] as

$$\begin{aligned} T_{\pm}(\eta) &= B_{\pm} D_{\pm\frac{ik^2}{2MH_0}}\left[(1\mp i)\sqrt{MH_0}\eta\right] \\ &\quad \mp \frac{k}{2\sqrt{MH_0}}(1\pm i) B_{\mp} D_{\mp\frac{ik^2}{2MH_0}-1}\left[(1\pm i)\sqrt{MH_0}\eta\right] \end{aligned} \tag{30}$$

where Eq.(22) has been used to relate the constants of the two independent solutions. $\sqrt{MH_0}$ is the reciprocal of the geometric mean of the Hubble time of the Universe and the Compton time of the Dirac particle. From the discussions of the previous paragraph, we can fix the constants to be

$$B_{\pm} = \pm\frac{1}{\sqrt{2}} e^{-\frac{\pi k^2}{4H_0 M}}\left[D_{\mp\frac{ik^2}{2MH_0}}(0) \mp \frac{k(1\pm i)}{2\sqrt{H_0 M}} D_{\mp\frac{ik^2}{2MH_0}-1}(0)\right]$$

by requiring $T_{\pm}(0) = \pm\frac{1}{\sqrt{2}}$. The behaviour of the solutions Eq.(30) for some values of k are shown in Fig. (2 and 3).

Next, we try to approximate the solutions of Eq. (30) by WKB method, assuming that a changes very slowly with η so that $a'(\eta)$ is small, i. e. the expansion rate of the Universe is small compared to the size of the Universe. Multiplying the derivative in Eq.(22) with δ to incorporate the order of the approximation and substituting $T_{\pm} = \exp\left(-\frac{i}{\delta}\sum_{n=0}^{\infty}\delta^n \int f_n d\eta\right)$ in Eq. (28) we get the equation for f:

$$\sum_{n=0}^{\infty}\delta^n\left\{\sum_{m=0}^{n}\left(f_m f_{n-m} + i f'_{n-1}\right)\right\} = k^2 + M^2a^2 \mp i\delta M a'. \tag{31}$$

Equating equal powers of δ we get the equations for the respective orders of the approximations:

$$\begin{aligned} f_0 &= \sqrt{k^2 + M^2a^2} = a\varepsilon_0, \\ 2f_0 f_1 &= -i\left(f'_0 \pm Ma'\right) \text{ and} \\ -if'_{n-1} &= \sum_{m=0}^{n} f_m f_{n-m}. \end{aligned} \tag{32}$$

Solving to the first order, we find $\int f_1 d\eta = i\ln\sqrt{1\mp\frac{M}{\varepsilon_0}}$, so we can write the solution to first order as

$$T_{\pm} = \pm\sqrt{\frac{\varepsilon_0 \mp M}{2\varepsilon_0}} e^{-i\int a\varepsilon_0 d\eta}, \tag{33}$$

which resembles the solution in Minkowskian space-time. The solution also gives us another important information, viz., at late times (in the evolution of the Universe) when $a \to \infty$, $\varepsilon_0 \to M$, so $T_+ \to 0$ and $T_- \to -1$. This shows that one of the solutions decays in time as the Universe expands, while the other solution grows. So, we suspect that the former one should be negative energy solution and the latter the positive energy solution because it is in consistent with the behaviors of the Dirac field in the Minkowski space where it is found that the negative energy solutions exist only in the relativistic regime while in the non-relativistic limit it is the positive energy solution that dominates [27]. However, it has to be confirmed with further investigations.

3 Particle Current and Energy-Momentum

The η and r components of the four-current integrated over the angular co-ordinates are found to be (with S defined in Eq. (2))

$$4\pi a^4 J^\eta S^2 = 4\pi n a^3 S^2 = \left[|R_+|^2 |T_+|^2 + |R_-|^2 |T_-|^2\right] = 4\pi S^3 a^3 (n_- + n_+)$$

$$\text{and} \qquad 4\pi a^4 J^r S^2 = -R_+^* R_- \left(T_+^* T_- - T_+ T_-^*\right) = -\frac{R_+^* R_-}{ik} \frac{d}{d\eta} |T_+|^2 \tag{34}$$

At this point, we are not much concerned with the other components, viz. $J^\theta \propto Y_+^* Y_- - Y_+ Y_-^* = 0$ and $a^4 J^\phi S^2 = -\frac{iR_+^* R_-}{2\sin\theta}\left(T_+^* T_- + T_+ T_-^*\right)\left(Y_+^* Y_- + Y_+ Y_-^*\right)$ which is independent of ϕ. The equation of continuity becomes $\frac{\partial}{\partial\eta} n a^3 S^2 = -\frac{\partial}{\partial r} a^4 S^2 J^r = \frac{1}{ik}\frac{dR_+^* R_-}{dr}\frac{d|T_+|^2}{d\eta}$ on using the relations Eq. (27). Integrating the comoving number density over the whole volume, the total number contained within the whole of the closed Universe gives us the normalization condition $N_T a^3 = \int_0^\pi dr \int n a^3 \sin^2 r d\Omega = |T_+|^2 + |T_-|^2 = 1$ so that the total comoving number is conserved. In the extreme relativistic regime, i.e., in very early epoch of the Universe, when its size was small ($a \to$ small), assuming a Fermi-Dirac(FD) type of distribution, and taking the volume of the closed space to be $V = \int_0^\pi S^2 dr \int d\Omega = 2\pi^2$, we may write the average number density of the particles as

$$n a^3 = \frac{1}{2\pi^2} \sum_{k,l,m} \frac{1}{e^{k+l+1}+1} = \frac{1}{2\pi^2} \sum_{k=0}^{\infty} \frac{(k+1)(k+2)}{e^{k+3/2}+1} = 0.0827975. \tag{35}$$

The FD value is $n a^3 = 0.0913454$, and this distribution deviates significantly from Fermi-Dirac at low n. The number distribution, corresponding to the massless case, is shown and compared with the FD distribution in Fig. (4).

On the other hand, integrating over the angular co-ordinates and only out

to a radius r, we have

$$\begin{aligned} Na^3 &= \int_0^r na^3 S^2\, dr\, d\Omega = \int_0^r |R_-|^2\, dr + \frac{R_+^* R_-}{ik} |T_+|^2 \\ &\to \int_0^r |R_-|^2\, dr + \frac{R_+^* R_-}{2ik} \left(1 - \frac{Ma}{\sqrt{k^2 + M^2 a^2}}\right), \\ &\quad 1^{\text{st}} \text{ order WKB} \end{aligned} \tag{36}$$

for the relative number of particles within a finite volume. This WKB result are plotted for representative cases in Fig. (5).

Particularly, for flat Universe, the comoving particle number and the particle current can be obtained using the expression for $R_\pm$ given by Eq. (26) and $T_\pm$ given by Eq. (30). Their sample plots have been shown in Figures (6), (7) (with different values of M) and (10) (with different values of conformal time η).

Next, we consider the energy-momentum tensor. At present we are concerned only with the $\eta\eta$ and rr components giving the density ρ and the pressure P_r respectively. After integration over the angular co-ordinates, we end up with

$$\begin{aligned} 4\pi S^2 \rho a^4 &= -\frac{k}{2}\left(|R_+|^2 + |R_-|^2\right)\left(T_+^* T_- + T_+ T_-^*\right) \\ &\quad - \left[Ma\left(|Z_+|^2 - |Z_-|^2\right)\right], \\ 4\pi S^2 P_r a^4 &= -\frac{1}{2}\left[k\left(|R_+|^2 + |R_-|^2\right) - \frac{(2l+1)}{\sin r}\frac{R_+^* R_-}{i}\right] \\ &\quad \times \left(T_+^* T_- + T_+ T_-^*\right), \\ &\text{and} \\ 4\pi S^2 (\rho - 3P) a^3 &= -M\left(|Z_+|^2 - |Z_-|^2\right). \end{aligned} \tag{37}$$

In the last equation for the trace, $3P = P_r + P_\theta + P_\phi$. Differentiating the energy density with respect to a we find the energy conservation law as

$$4\pi S^2 \frac{d}{da}\rho a^4 = -M\left(|Z_+|^2 - |Z_-|^2\right) = 4\pi S^2 (\rho - 3P) a^3. \tag{38}$$

WKB results for the quantities ρa^4 and $Ea^4 = 4\pi \int_0^r \mathrm{S}^2 \rho a^4 dr$ are shown in Fig. (11).

Comparing Eq. (38) with Eq. (34), it is important to note that

$$4\pi S^2 n a^3 = |R_- T_-|^2 + |R_+ T_+|^2$$

$$and\ 4\pi S^2 \frac{d(\rho a^4)}{d(aM)} = |R_- T_-|^2 - |R_+ T_+|^2 = 4\pi S^2 a^3 (n_- - n_+)$$

so that the rate of energy density change per unit mass is equal to the difference in the comoving particle number density of the '-' and '+' states.

From Eq. (38), $d\left(\rho a^3\right) = -Pda^3$, which is the Second Law of Thermodynamics for adiabatic expansion. This equation can be processed to give the time independent entropy

$$\mathcal{S}(r) = \frac{a^3(\rho + P)}{T}. \tag{39}$$

The total energy inside the closed Universe is

$$\begin{aligned} Ea^4 &= \int_0^\pi dr \int \rho a^4 \sin^2 r d\Omega \\ &= -k\left(T_+^* T_- + T_+ T_-^*\right) - Ma\left(|T_+|^2 - |T_-|^2\right). \end{aligned} \tag{40}$$

Dividing this by the conserved comoving total number $Na^3 = 1$, and using similar process with Eq. (38), we get the equations for the average comoving energy of one Dirac particle and its time evolution:

$$\varepsilon a = -k\left(T_+^* T_- + T_+ T_-^*\right) - Ma\left(|T_+|^2 - |T_-|^2\right) \text{ and} \tag{41}$$

$$\frac{d\varepsilon a}{da} = -Ma\left(|T_+|^2 - |T_-|^2\right). \tag{42}$$

Eqs.(41 and 42) allow us to write

$$2M|T_\pm|^2 = M \mp \frac{d\varepsilon a}{da} \text{ and} \tag{43}$$

$$k\left(T_+^* T_- + T_+ T_-^*\right) = a^2 \frac{d\varepsilon}{da}. \tag{44}$$

We can also express the evolution of the moving energy in any Friedmann type model by the equation

$$\left(a' \frac{d}{da} a' \frac{d}{da} + 4k^2 + 4M^2 a^2\right) \frac{d\varepsilon a}{da} - 4M^2 a(\varepsilon a) = 0. \tag{45}$$

Eq. (45) can be solved, at least numerically or by series method, for any behaviour of a.

For the flat Universe, the energy density and rate of flow of energy can be obtained explicitly as we did for particle number, by using the expression for $R_\pm$ given by Eq. (26) and $T_\pm$ given by Eq. (30) in Eq. 40 . The plots of these for some representative cases have been shown in Figs. (12), (13) and (14).

$$\begin{aligned} \frac{1}{\dot{a}} \frac{\partial(Ea^4)}{\partial \eta} = \frac{\partial(Ea^4)}{\partial a} &= |A_\pm|^2 \left[\frac{M}{2k}\left(|T_+|^2 - 1\right) r^2 j_{l-1/2} j_{l+1/2}\right] \\ &+ |A_\pm|^2 \frac{M}{2}\left(1 - 2|T_+|^2\right) \int_0^r \left(r\, j_{l+1/2}\right)^2 dr \end{aligned} \tag{46}$$

4 Conclusions

In this work, we have investigated the behaviour of the Dirac field in closed FRW spacetime using NP formalism - spinor analysis. This work has two important aspects. One is the method itself; we want to illustrate the fact that the NP formalism is a very powerful and convenient method to study the behaviour of spin fields in curved background spacetime. It yields more tractable equations for the eigenfuctions compared to the conventional tensorial method. It appears to be more natural as it goes into very quantal nature of the fields as illustrated by its ability to explain the absence of super-radiance of neutrinos in Kerr spacetime[7]. Another aspect is the solution of the field equations itself that have become more transparent in revealing the nature of the distributions of the particles and energy. Ultimately all matter is fermionic, so behaviour of Dirac field in expanding Universe must reveal the unknown features of the Universe and also unleash some facts about structure formation.

While the free Maxwell and Dirac fields, in Friedmann-Robertson-Walker spacetime were investigated using the Newman-Penrose method, all the variables were found to be separable, and the angular solutions were the spin-weighted spherical harmonics. The massless fields came to have the usual exponential time dependencies. All the radial parts reduced to the quantum mechanical barrier penetration problem, with well behaved potentials that are basically the centrifugal energies. The potentials seen by one component of the Dirac field, R_+, are interesting; its lowest angular momentum state sees no potential in the flat universe, while it sees an attractive one throughout the open universe; from afar, all angular momentum states of this component see attractive potential in the open universe. Consequences of this effect may provide a means to determine whether the Universe is flat, open or closed. All the radial equations are solved.

We have looked into the properties of the massive Dirac field in detail for closed FRW spacetime. The radial dependence in the open Universe is also the appropriate limit. The flat case can be considered to be the limit of either the closed or open cases for $K \to 0$. Thus, in the complexified r-plane, the closed Universe lies along the real axis, open along the imaginary and flat near the origin. So, we may consider the proposition that, as an overall flat space expands, it fragments into under-density voids that develop locally as an open FRW space along the imaginary axis, and the overdensity regions evolve locally into the large scale structures as the closed counterpart. Hence the closed, open and flat Universes represent different regions of a complexified space.

The radial dependence is the same for both the massless and massive cases. The momentum is quantized in steps of unity from the minimum value of 3/2. The quantization condition for the comoving mementum of a gravitationally trapped Dirac particle is $k = l + \mathrm{n} + 1$, where $\mathrm{n} \geq 0$ is an integer, and the total angular momentum l is a half integer.

The temporal solution (Eq. 33) gives us an important information, viz,. at late times of the evolution / expansion of the Universe when $a \to \infty$, $\varepsilon_0 \to M$, so $T_+ \to 0$ and $T_- \to -1$, showing that one of the solutions decays in

time as the Universe expands, while the other solution grows. This leads us to conclude that the former one may be the negative energy solution while the latter is the positive energy solution. This will be confirmed in future work on the representation of the Dirac matrices. The variations in number densities exist from the very initial time of the big-bang. There was indication from our early work [17] that, although the comoving number density of the massless field is locally conserved at every spacetime point, it is not so for the massive case. Even though the Universe starts out with equal number of particles with $|T_+|^2 = |T_-|^2 = 1/2$, at late times the former goes down towards zero while the latter grows to unity keeping the sum conserved and equal to unity. As the universe expands and the particles lose their kinetic energy, the time dependence shows that the $|Z_+T_+|^2$ representing the number of particles in this model will decay while $|Z_-T_-|^2$ grows. This may be mimicking the behavior of the massive Dirac field in Minkowski spacetime where the negative energy solutions exist only in the relativistic regime while the positive energy solution dominates in the non-relativistic regime.[27]. This could be the source of the local particle current that exists at every point in the FRW spacetime. Nonetheless, the total comoving number within the whole volume is still conserved. Further, the currents are set up in such a way that the over-densities are further enhanced while the under-densities get more depleted as the Universe expands.

The energy distribution also follows the number distribution. We find that the number and energy distributions that are setup have exactly the same form as required by the flat ratation curves of galaxies. The Newtonian gravitational potential that is required for the flat rotation curve is that the square of the rotational velocity of the particles, $v^2 \propto \frac{M(r)}{r} \propto \frac{N(r)}{r} = \text{constant}$. Our results also show that the plots of the quantities $\frac{E(r)}{r}$ and $\frac{N(r)}{r}$ become flat at a short distance from the origin as the Figs. (5 and 11) show. Even the surface densities of particles and energy at a distance r show the same nature. The particle number and energy distributions have also been plotted for different masses and different conformal times (in the units of Hubble time) and it is seen that density contrast is enhanced for larger mass M as well as with the elapse of time as expected.

The over- and under-density fluctuations that exist from the very begining further get enhanced with the expansion of the Universe. As a consequence, fragmentation can be induced as the underdensity regions inbetween the over-densities become highly depleted. The angular-momentum contained by these structures must also be the source of rotation of galaxies and clusters. As our Universe is almost flat, any gravitationaly bound large scale structure will mimic a closed Universe.

This work has to be continued further, and these preliminary results confirmed by simulation. Also, quantization of the Dirac field must be done and the corrections accounted for conclusive arguments. Another extension would be the study of quantum electrodynamics of the interacting Dirac and Maxwell fields.

References

[1] B. van der Waerden and Gottinger Nachichten, *Spinor Calculus*, (Leipzig, 1929) p. 100; M. R. Schneider, *B. L. van der Waerden's early contribution to quantum mechanics*, (Leipzig, 2008).

[2] V. Fock, *Zeits. f. Physik* **57**, 261 (1929).

[3] O. Laporte and G. E. Uhlenbeck, *Phys. Rev.* **37**, 1380 (1931).

[4] P. A. M. Dirac, *Proceedings of the Royal Society of London* **155**, 447 (1936).

[5] D. R. Brill and J. A. Wheeler, *Rev. Mod. Phys.* **29**, 465 (1957).

[6] E. T. Newman and R. Penrose, *J. Math. Phys.* **3**, 566 (1962).

[7] S. Chandrasekhar, *The Mathematical Theory of Black Holes*, (Clarendon Press, Oxford, 1983).

[8] D. Lohia and N. Panchapakesan, *J. Phys. A* **11**, 1963 (1978); **12**, 533 (1979)

[9] U. Khanal and N. Panchapakesan, *Phys. Rev. D* **24**, 829 and 835 (1981); Annals of Phys. **138**, 260 (1982).

[10] B. Mukhopadhyay and N. Dadhich, *Class. Quantum. Grav.* **21,** 3621 (2005).

[11] U. Khanal, *Phys. Rev.* **28**, 1291 (1983); **32**, 879 (1985).

[12] N. Haghighipour, arXiv: gr-qc/0405140; *Gen. Relativ. Gravit.* **37**, 327 (2005).

[13] M. Sharif, *Chin. J. Phys.* **40**, 526 (2002); arXiv: gr-qc/0401065.

[14] J. Bicak and J. Slavik, *Acta. Phys. Pol.* **B6**, 489 (1975).

[15] A. Al-Badawi and I. Sakalli, arXiv: 0805.4485.

[16] A. Zecca, *J. Math. Phys.* **37**, 874 (1996)*; Adv. Stud. Theor. Phys.* **3**, 239 (2009).

[17] U. Khanal, *Class. Quantum. Grav.* **23,** 4353 (2006).

[18] U. Khanal, *ICTP* IC/2006/136P.

[19] E. W. Kolb and M. S. Turner, *The Early Universe*, (Addison-Wesley, New York, 1990).

[20] S. Weinberg, *Cosmology,* (Oxford Press, Oxford, 2008).

[21] A. O. Barut and I. H. Duru, *Phys. Rev.* **D 36**, 3705 (1987).

[22] A. Zecca, *Nuovo Cimento* **B113**, 915 (1998).

[23] A. Zecca, *Int. Jour.Theoret. Phys.* **45**, 44 (2006).

[24] X. B. Huang, arXiv: gr-qc/0501077.

[25] M. Abramowitz and I. A. Stegun, *Handbook of Mathematical Functions,* New York, Dover (1976).

[26] I. S. Gradshteyn and I. M. Ryzhik, *Table of Integral, Series and Products*, (Academic Press, New York, 1980).

[27] P. Roman, *Advanced Quantum Theory: An outline of fundamental ideas,* , (Addision-Wesley, Reading, USA, 1965).

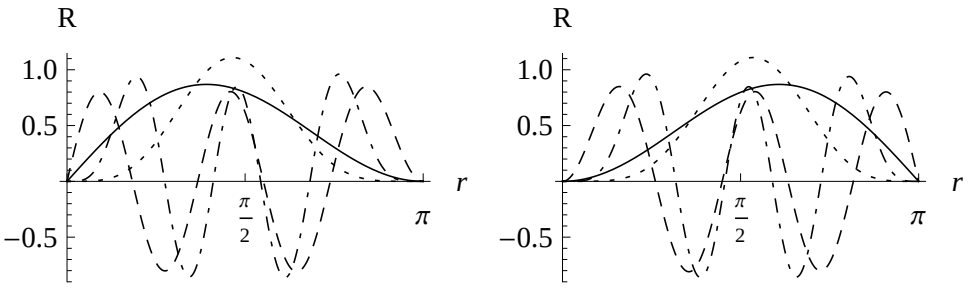

Figure 1: The radial dependence, R_+ on the right and R_-/i on the left. The $l = 1/2$, are filled for $k = 3/2$ and dotted for $5/2$ respectively; the $l = 7/2$ are dashed for $k = 11/2$ and dot-dashed for$k = 17/2$.

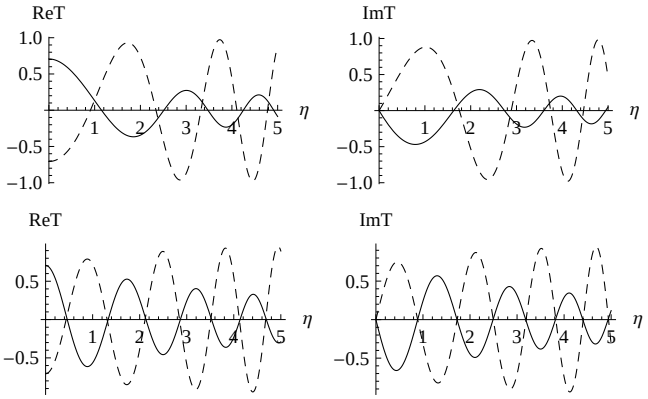

Figure 2: The temporal dependence of the Dirac field in a radiation filled flat FRW space-time. T_+ are shown by solid and T_- by dashed lines respectively. The upper two are real and imaginary parts for $\frac{k}{\sqrt{H_0 M}} = \frac{3}{2}$, and the lower two for $\frac{k}{\sqrt{H_0 M}} = \frac{7}{2}$.

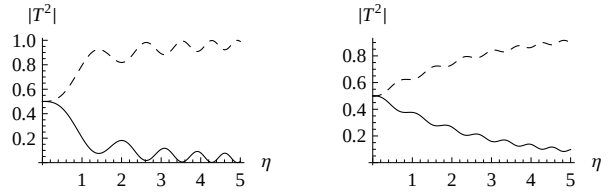

Figure 3: Solid curves are$|T_+|^2$, and dashed are$|T_-|^2$; $\frac{k}{\sqrt{H_0 M}} = \frac{3}{2}$ are at the left and $\frac{k}{\sqrt{H_0 M}} = \frac{7}{2}$ at the right. $|T_+|^2$ are seen to decay to zero while$|T_-|^2$ grow to unity.

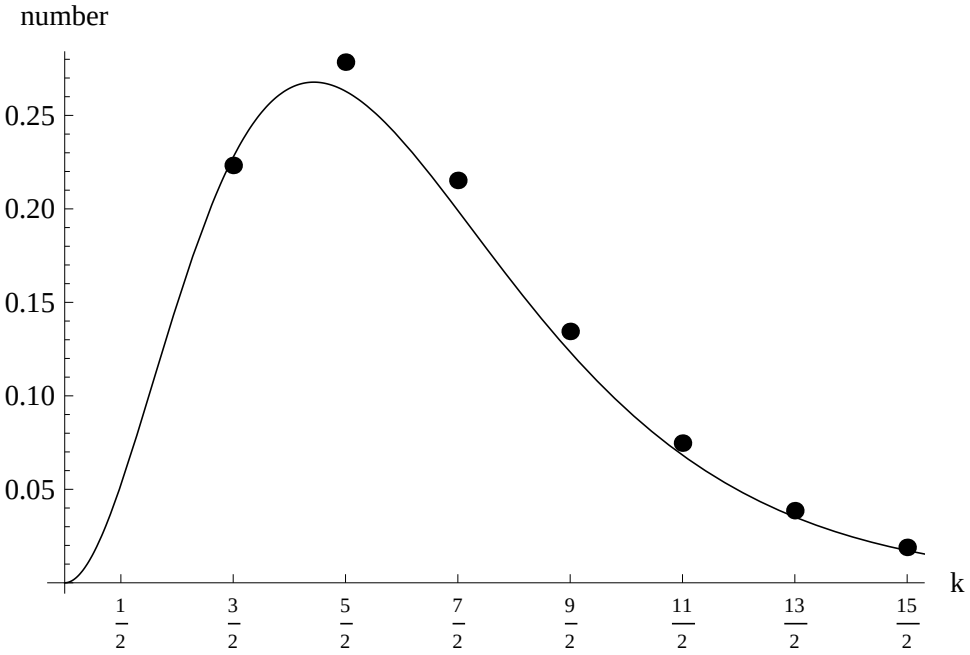

Figure 4: The relative particle number distribution of extremely relativistic fermions in closed FRW space. The momentum k is quantized upwards in steps of unity from the minimum value of $3/2$, and the filled dots represent the relative number of particles with that momentum. The filled curve is the Fermi-Dirac distribution. We see that at low momenta, the distribution is quite different, but for high k the two start to coincide.

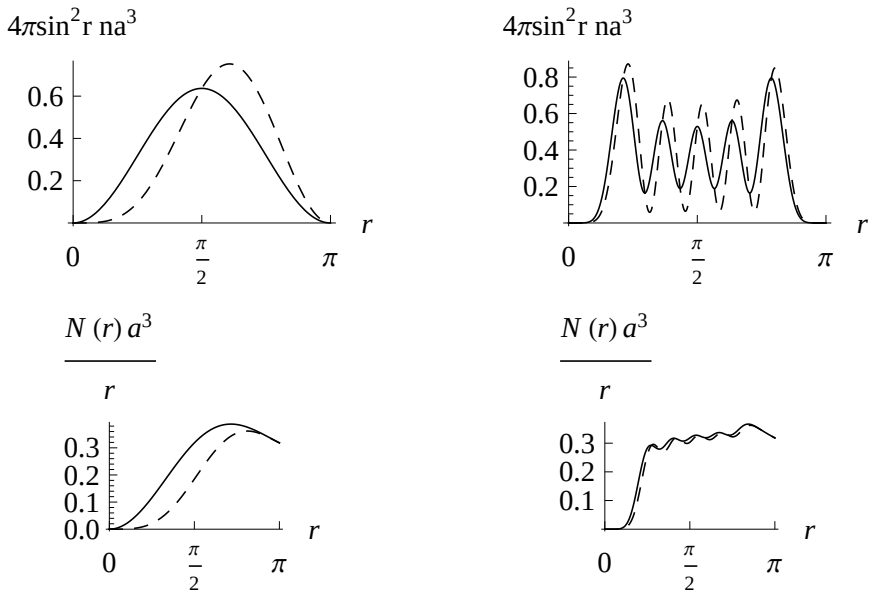

Figure 5: The number of Dirac particles in closed FRW space-time. The upper two are the local surface densities of particle number, and the lower two are the total number divided by r. On the left are $k = 3/2$, $l = 1/2$, and on the right are $k = 17/2$, $l = 7/2$. Solid curves are the respective quantities at the instance of the big bang when $a = 0$, and the dashed at $a = 10$. It is seen that as the Universe expands, the density contrast become more enhanced. The lower graphs show that the particle distribution has the same behaviour as that demanded by the flat rotation curves of galaxies.

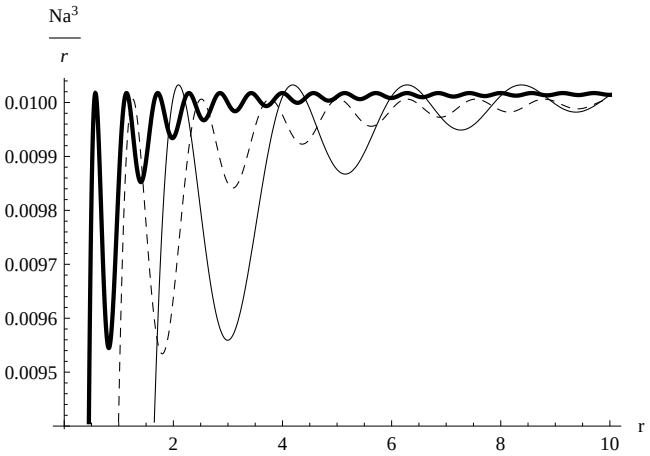

Figure 6: The comoving particle number (Na^3/r) for flat Universe at $\eta \to 0$. The normal solid line, dashed line and thick solid line are for k = 3/2, 5/2 and 11/2 respectively, all of which are for $l = 1/2$. They are appropriately scaled for comparision purpose. The quantities are found to saturate to a constant value resembling to the flattening of the rotation curves of galaxies.

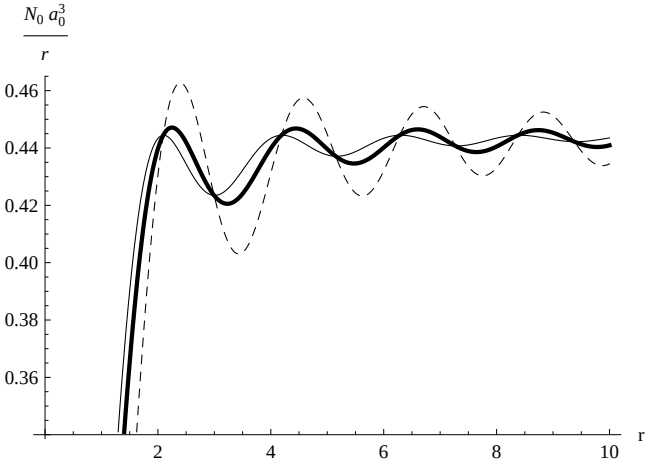

Figure 7: The comoving particle number (Na^3/r) for massive flat FRW spacetime with $l = 1/2$ and k = 3/2. The normal solid, dashed and thick solid curves are for M =0.01, 1 and 100 respectively. The behaviour is same as in the case of massless field except that amplitude of fluctuations are larger, and increase for increasing mass. The graphs for the three cases have been appropriately scaled to make of almost equal heights for comparision.

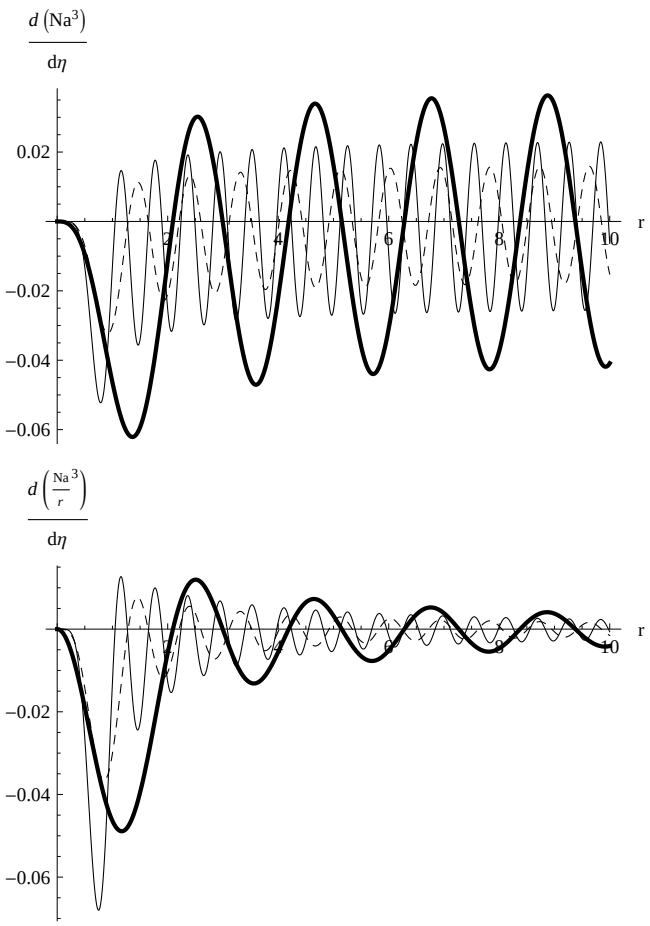

Figure 8: The comoving particle current for given mass and conformal time in flat FRW space time. The thick solid curve is for $l = 1/2$ and k = 3/2; the dashed curve is for $l = 3/2$ and k = 7/2; and normal solid curve is for $l = 5/2$ and k = 11/2. The lower one is the particle number divided by r. The later graphs show that the particle distribution has the same behaviour as that demanded by the flat rotation curves of galaxies.

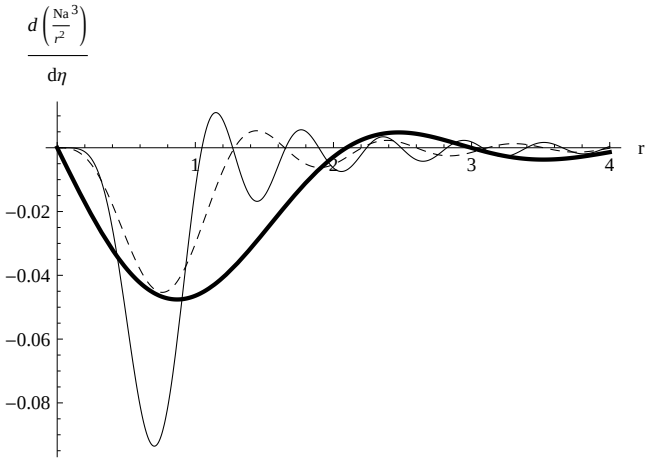

Figure 9: The rate of flow of comoving particles through a unit surface at r in flat FRW space time. The thick solid curve is for $l = 1/2$ and k = $3/2$; the dashed curve is for $l = 3/2$ and k = $7/2$; and normal solid curve is for $l = 5/2$ and k = $11/2$.

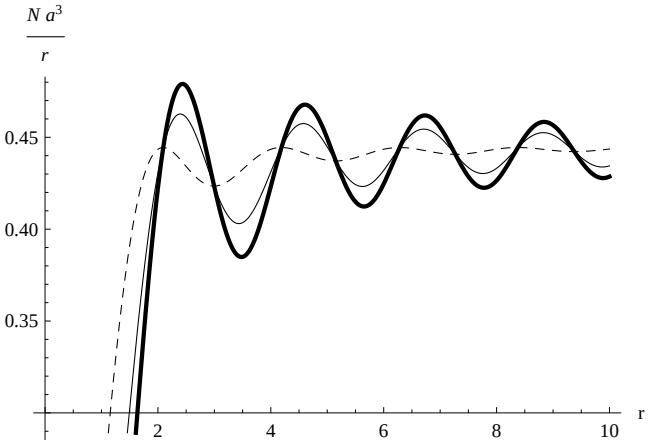

Figure 10: Evolution of Na^3/r at different conformal times η for M = 1. The normal solid curve is for $\sqrt{MH_0}\eta = 1$, the dashed curve is for $\sqrt{MH_0}\eta = .01$ and the thick solid curve is for $\sqrt{MH_0}\eta = 10,000$. All the graphs are for $l = 1/2$ and k = $3/2$. It is seen that the density contrast increases with the elapse of time.

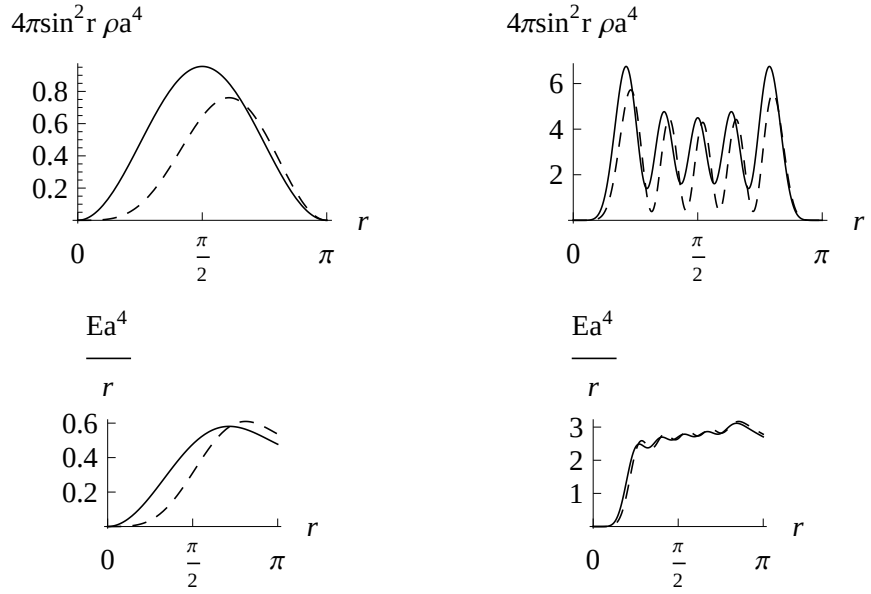

Figure 11: The energy of the Dirac field for the same values of k and l as in Fig. (5). But here the values are scaled for $a = 0$ and $a = 10$ to appear to be almost equal so that they can be compared. The energy follows the particle number as it should.

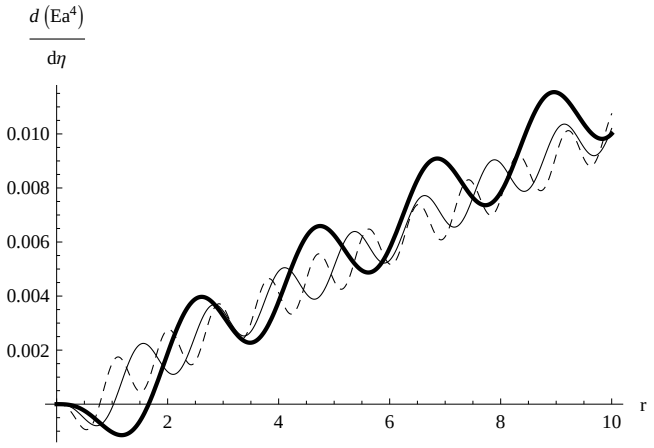

Figure 12: Comoving energy flow rate for flat universe at a given time and mass. Thick solid, dashed and normal solid lines are for k =3/2, 5/2 and 7/2 respectively. All are for $l = 1/2$.

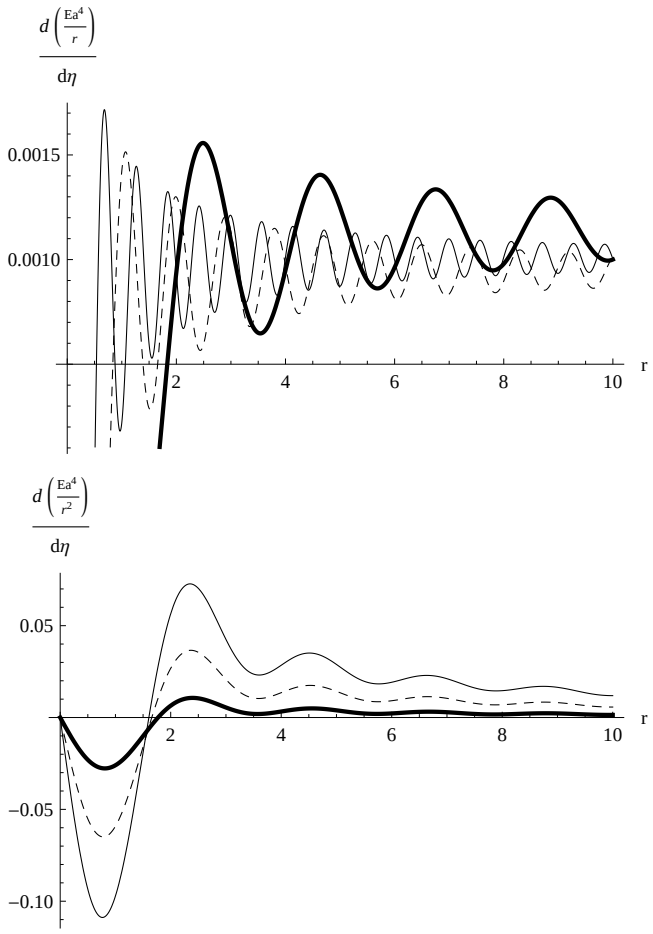

Figure 13: Rate of flow of comoving energy for the flat universe. The upper one is the energy divided by r and lower one is the energy flowing out of a unit surface area at a distance r. All are for $l = 1/2$ with k =3/2, 5/2 and 7/2 represented by thick solid, dashed and normal solid lines respectively

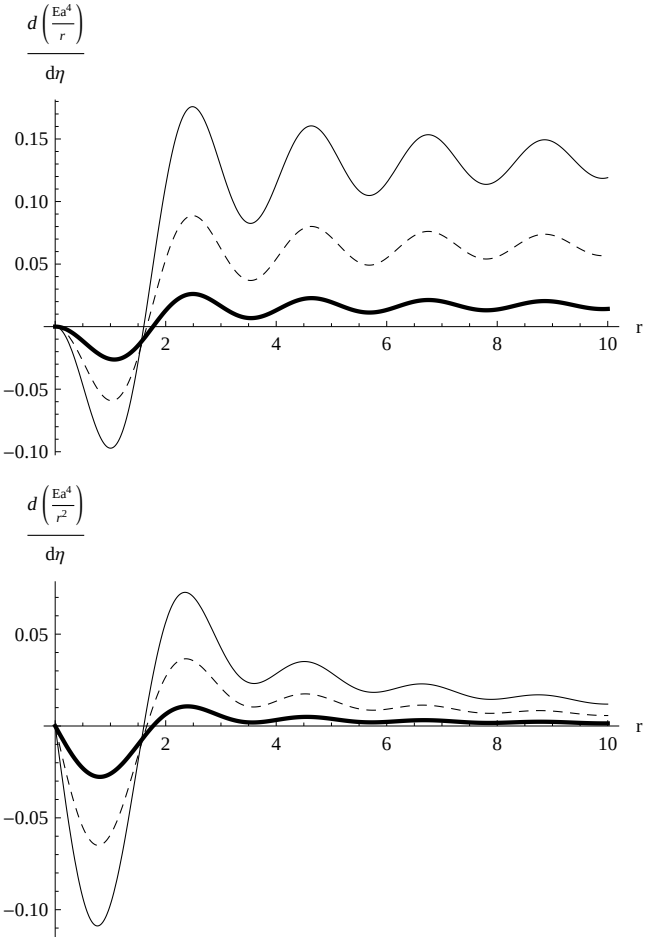

Figure 14: As in the figure - 13 for $l = 1/2$ and k = 3/2 with different M. Thick solid, dashed and normal solid lines are for M = 0.5, 1 and 1/5 respectively.